Spin distribution of compound nucleus formed by near-barrier fusion

B. T. Kim,* T. Udagawa, and T. Tamura
Department of Physics, University of Texas, Austin, Texas 78712
(Received 21 August 1985)

Spin distributions of compound nuclei formed by heavy-ion fusion reactions near the barrier are calculated, based on a direct reaction description we recently developed. The mean values of the distributions thus calculated are found to fit the observed data very well.

Within the framework of direct reaction (DR) theories,[1] the fusion process accounts for part of the imaginary term, W, of the optical potential. It seems natural to consider that the innermost portion of $W(r)$ is mainly due to fusion. Such an idea seems to have been around for a long time. Nevertheless, no serious attempt had been made to calculate fusion cross section based on such an idea.

We have recently formulated such calculations.[2-4] In that work, we introduced a fusion potential, $W_F(r)$, defined as the inner portion of W, i.e., the part with $r < R_F$, R_F being called the fusion radius. We then evaluated the fusion cross section σ_F as an expectation value of W_F with respect to a DR wave function, $\psi_a^{(+)}$. More concretely, σ_F was given as[2,4]

$$\sigma_F = (2\pi/\hbar v_a)(\langle \psi_a^{(+)} | W_F | \psi_a^{(+)} \rangle / \pi) \ , \tag{1}$$

where v_a is the relative incident velocity. In the simplest treatment, $\psi_a^{(+)}$ can be taken as the usual optical-model wave function. When coupling with some DR channels play an important role, a coupled-channel (CC) wave function that takes into account the coupling has to be used for $\psi_a^{(+)}$. In this case, W_F in Eq. (1) has to be considered as an operator, which has both diagonal and nondiagonal matrix elements with respect to the channel states.

As emphasized in Ref. 4, σ_F, as given by Eq. (1), includes DR effects via those included in $\psi_a^{(+)}$. There are two types of DR effects, i.e., those included explicitly in the CC calculations, and the rest. Since the number of coupled channels that we can take into account explicitly is quite restricted, the major part of the coupled-channel effects are not included explicitly. Now in $\psi_a^{(+)}$, we include both types of DR effects. Particularly, the second type of effect (the effects that are not taken into account explicitly) is accounted for via the use of the *full imaginary potential* W in obtaining $\psi_a^{(+)}$. This is clear from the fact that the W include the effects of DR as well as those of fusion. As discussed in detail in Ref. 4, we were able to reproduce very well the experimental σ_F in both the subbarrier- and above-barrier region and for a variety of systems, including those of very heavy systems, for which, e.g., the conventional barrier penetration model (BPM)[5] does not work.

It was also emphasized[4] that the DR method predicted a spin distribution (equivalently, the partial fusion cross section, $\sigma_F^{(J)}$) in the fused system that is very different from what was predicted, e.g., by BPM. It is thus interesting to test the calculated spin distributions against experimental data, e.g., the mean values $\langle J \rangle$ of the spin distributions, which have become available recently through measurements[6,7] of multiplicity of γ rays emitted from the fused systems. We aim at this in the present paper.

The mean value $\langle J \rangle$ of the spin distribution may be given in terms of $\sigma_F^{(J)}$ as

$$\langle J \rangle = \sum_J J \sigma_F^{(J)} / \sigma_F \ , \tag{2}$$

where $\sigma_F^{(J)}$ is explicitly written as[2,4] (for the general CC case)

$$\sigma_F^{(J)} = (8/\hbar v_a) \sum_{ll'l'} \int_0^\infty [\psi^J_{l'l'}(r)]^* W_{F;l'l'}(r) \psi^J_{ll}(r) \, dr \ , \tag{3}$$

where ψ^J_{ll} is the partial CC distorted wave function,[8] I, l, and J standing for the spin of the target, the orbital angular momentum, and the total angular momentum, respectively.

As in Refs. 2–4, we choose $W_F(r)$ as

$$W_F = \begin{cases} W, & (r < R_F) \ , \\ 0, & (r \geq R_F \ , \end{cases} \tag{4a}$$

with

$$R_F = r_F(A_1^{1/3} + A_2^{1/3}) \ . \tag{4b}$$

Here we assume that fusion takes place only inside R_F. In Ref. 4, we treated R_F (or equivalently r_F) as an adjustable parameter, and analyzed a number of experimental data for systems both below and above the barrier. The results of such analysis showed that the calculated σ_F, which we call $\sigma_F^{\rm DR}$ henceforth, fits the experimental data very well. The average value of r_F turned out to be $r_F = 1.46$ fm. This value was used as a guide for choosing the r_F value to be used in the present calculations.

We consider first data for the $^{16}O + ^{154}Sm$ system, taken by Vandenbosch *et al.*[6] Since the target (^{154}Sm) is deformed, the coupling with the 2^+ rotational channel[9] plays an essential role,[4] and we performed CC calculations. The details of the calculations are the same as those reported in Ref. 4. The same optical potential and fusion radius parameters as used in Ref. 4 were used in the present calculations.

In Fig. 1, both the calculated and experimental σ_F and $\langle J \rangle$ (denoted as $\langle J \rangle^{\rm DR}$ and $\langle J \rangle^{\rm exp}$, respectively) are presented as functions of the incident energy, $E_{\rm cm}$. The full lines shown there are the results of the present calculations, while the dotted line shown for $\langle J \rangle$ is that of the sharp cutoff model (scm), i.e., $\langle J \rangle^{\rm scm} = (\frac{2}{3}) J_{cr}$, with $J_{cr} = (k_a^2 \sigma_F / \pi)^{1/2} - 1$.

As seen in Fig. 1, $\sigma_F^{\rm DR}$ fits $\sigma_F^{\rm exp}$ very well. The overall fit of $\langle J \rangle^{\rm DR}$ to $\langle J \rangle^{\rm exp}$ is also fairly good. We notice, however, that $\langle J \rangle^{\rm DR}$ is slightly larger (by about one unit) than $\langle J \rangle^{\rm exp}$ is. In fact, if the whole experimental result were to be moved up by one unit, the fit would become excellent.

In connection with this, it is worth noticing that in ex-

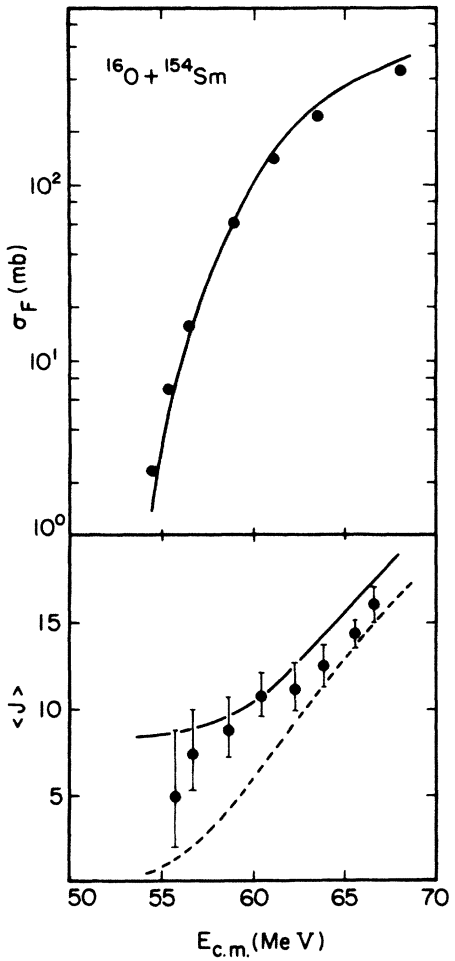

FIG. 1. Comparison with calculated and experimental fusion cross sections (σ_F) and average spin of the compound nucleus ($\langle J \rangle$) for the $^{16}O+^{154}Sm$ system. The solid circles are experimental σ_F and $\langle J \rangle$, while the full lines represent calculated σ_F and $\langle J \rangle$. The dotted line shown for $\langle J \rangle$ is calculated $\langle J \rangle$ from the sharp cutoff model.

tracting the $\langle J \rangle^{exp}$ values from the measured γ-ray multiplicity, no account was taken of the angular momentum, J_{xn}, taken away by evaporated x neutrons, where x stands for the number of neutrons evaporated. For the energy region considered here, x is 2–4. Very accurate information of J_{xn}/x is not known in this energy region. However, statistical model calculations[10] done so far suggest that J_{xn}/x is in the range 0.2–1.0, depending on the energy and the projectile.[10] Therefore, it is quite probable that the actual $\langle J \rangle^{exp}$ values are larger than those given in Ref. 6, improving the fit of $\langle J \rangle^{DR}$ with $\langle J \rangle^{exp}$.

It is also notable that $\langle J \rangle^{DR}$ are systematically larger than $\langle J \rangle^{scm}$ for all the energies considered. A large difference between $\langle J \rangle^{DR}$ and $\langle J \rangle^{scm}$ seen at lower energies (below the barrier) may be due to Coulomb barrier penetration. We shall argue later that the difference seen at the above-barrier region can be ascribed to the DR effect.

As the next example, we consider systems for which data were taken by Haas *et al.*[7] In Ref. 7, data were taken for the $^{16}O+^{144}Nd$, $^{37}Cl+^{123}Sb$, $^{64}Ni+^{96}Zr$, and $^{80}Se+^{80}Se$ systems. These systems all lead to the same compound nucleus ^{160}Er. The data were taken at three different incident energies near the barrier, for each system, the energies being chosen so as to produce ^{160}Er at the same excitation energies of $E^*=48.5$, 53.5, and 58.5 MeV.

Since none of the ions involved has a specific nuclear structure that requires one to perform CC calculations, all the calculations were done without including any CC effect. Unfortunately, for none of the systems is the optical model potential known. Therefore, the parameters were taken as those used in Ref. 4 for the nearest neighbors, i.e., the $^{16}O+^{148}Sm$, $^{40}Ar+^{122}Sn$, $^{64}Ni+^{58}Ni$, and $^{58}Ni+^{58}Ni$ systems, respectively, for the four systems mentioned above. Also, the fusion radius parameters were fixed so that σ_F^{DR} fits to σ_F^{exp} as well as possible. (The values thus fixed were $r_F=1.39$, 1.44, 1.42, and 1.45 fm for the $^{16}O+^{144}Nd$, $^{37}Cl+^{123}Sb$, $^{64}Ni+^{96}Zr$, and $^{80}Se+^{80}Se$ systems, respectively.)

In Fig. 2, both calculated and experimental σ_F and $\langle J \rangle$ are plotted as functions of E_{cm}. We also present there the values of $\langle J \rangle^{scm}$ by dotted lines. As seen, the overall fit to the data is very good for both σ_F and $\langle J \rangle$. One remarkable feature of the experimental data is that they show a very strong entrance channel effect; i.e., the values depend rather strongly on the system, in spite of the fact that E^* of the compound nucleus formed is the same. For instance, σ_F of the $^{16}O+^{144}Nd$ system is much larger than those of the other three systems. Also $\langle J \rangle^{exp}$ increases gradually as the mass of the incident ion increases. All these features are well reproduced by our calcultions. It is also notable that

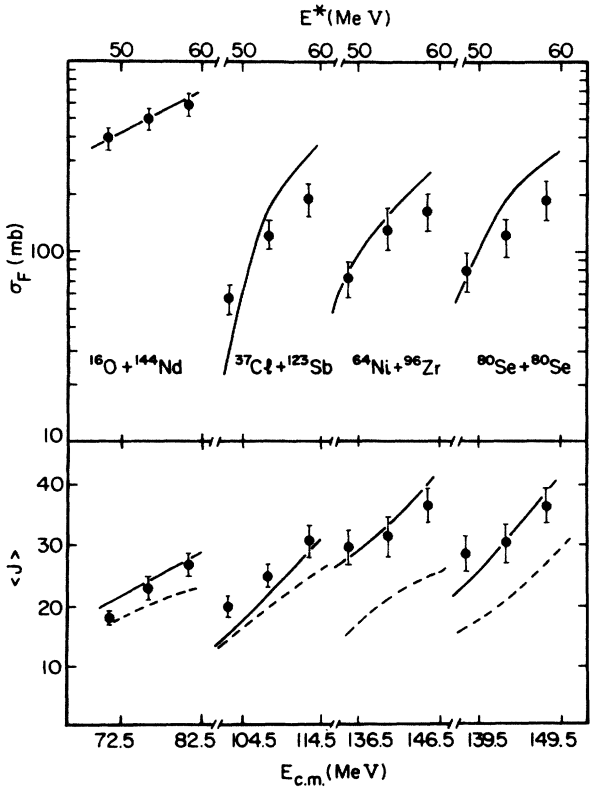

FIG. 2. Comparison with calculated and experimental fusion cross sections (σ_F) and the average spin of the compound nucleus ($\langle J \rangle$) for the $^{16}O+^{144}Nd$, $^{37}Cl+^{123}Sb$, $^{64}Ni+^{96}Zr$, and $^{80}Se+^{80}Se$ systems. The rest is the same in Fig. 1.

$\langle J\rangle^{\rm scm}$ is systematically smaller than $\langle J\rangle^{\rm DR}$ and $\langle J\rangle^{\rm exp}$.

In order to obtain a more detailed insight into the above entrance channel dependence, we present in Fig. 3 the calculated $\sigma_F^{(J)}$ as a function of J for all the four systems considered above, restricting here, however, only to the highest incident energy cases. We also present in Fig. 3 calculated partial reaction cross sections, $\sigma_R^{(J)}$. It should be noticed that the calculated $\sigma_R^{(J)}$ values were essentially equal to the geometrial (scm) value of $(\pi/k_a^2)(2J+1)(=\sigma_{\rm scm}^{(J)})$, particularly at lower J.

A remarkable feature seen in Fig. 3 is that $\sigma_F^{(J)}$ is significantly smaller than is $\sigma_R^{(J)}$, even for lower J. This explains why $\langle J\rangle^{\rm DR}$ is generally larger than is $\langle J\rangle^{\rm scm}$. Since the difference between $\sigma_R^{(J)}$ and $\sigma_F^{(J)}$, i.e., $\sigma_{\rm DR}^{(J)}=\sigma_R^{(J)}-\sigma_F^{(J)}$, is nothing but the DR cross section, we may say that the above reduction of $\sigma_F^{(J)}$ from $\sigma_R^{(J)}$, and also the shift of $\langle J\rangle^{\rm DR}$ from $\langle J\rangle^{\rm scm}$ towards larger values is caused by the DR effects. As discussed before, a similar shift of $\langle J\rangle^{\rm DR}$ was also obtained in the ^{16}O+^{154}Sm system, which may similarly be explained as due to the DR effects.

In Fig. 3, it is also seen that the total area of the $\sigma_F^{(J)}$ distribution (i.e., σ_F) for the ^{16}O+^{144}Nd system is particularly large as compared with those for the rest of the systems. This is due to the fact that $E_{\rm cm}$ for this system is particularly higher than is the barrier; in fact, $E_{\rm cm}$ for this system is about 20 MeV above the barrier, while $E_{\rm cm}$'s for the rest of the systems are all 10 MeV above the barrier. This explains why the ^{16}O+^{144}Nd system has particularly a large σ_F value.

Among the rest of the cases, the ^{64}Ni+^{96}Zr and ^{80}Se+^{80}Se systems have almost the same $\sigma_F^{(J)}$ and $\sigma_R^{(J)}$ distributions. The distributions of the ^{37}Cl+^{123}Sb system is, however, rather different from those of the above two systems. The $\sigma_F^{(J)}$ distribution, say, for the ^{64}Ni+^{96}Zr system has a distribution which is much more flattened than that for the ^{37}Cl+^{123}Sb system. This entrance channel dependence for the DR effects explains why $\langle J\rangle^{\rm DR}$ for the former system is much larger (by about 6 units) than that for the latter system.

The flattening of the $\sigma_F^{(J)}$ distributions is caused by DR effects, and what we observed above indicates that the DR effects play a more important role in the ^{64}Ni+^{96}Zr system than in the ^{37}Cl+^{123}Sb system. This entrance channel dependence of the DR effects may be understood in terms of the Coulomb effect. Note that the Coulomb force in the former system is considerably larger than that of the latter system. The trajectories with smaller impact parameters are thus pushed away more towards the peripheral region in the former case than in the latter. This increases the chance that the direct reactions will take place, even for lower partial waves, in the former system as opposed to the latter system.

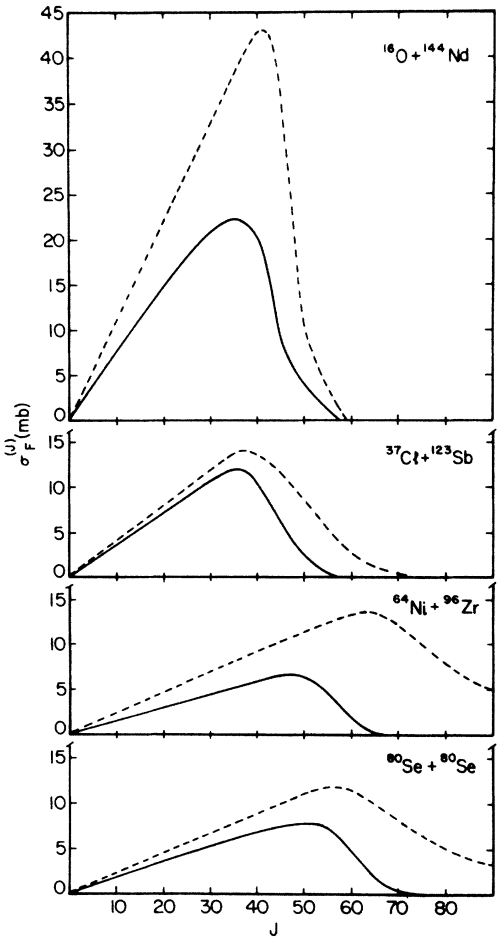

FIG. 3. Calculated partial fusion (solid curves) and reaction (dashed curves) cross sections for the ^{16}O+^{144}Nd, ^{37}Cl+^{123}Sb, ^{64}Ni+^{96}Zr, and ^{80}Se+^{80}Se systems for $E_{\rm cm}=82.5$, 114.5, 146.5, and 149.5 MeV, respectively.

In summary, we tested the spin distributions, calculated from the theory proposed recently, against the measured mean spin values. The calculated mean values fitted the data very well, indicating that the theory works also for predicting the spin distributions of the compound system.

This work was supported in part by the U.S. Department of Energy, and also by the Ministry of Education, Korea, through the Basic Science Research Institute Program.

*Permanent address: Department of Physics, Sung Kyun Kwan University, Suwon, Korea.

[1]N. Austern, *Direct Nuclear Reaction Theories* (Wiley, New York, 1970); G. R. Satchler, *Direct Reaction Theories* (Oxford Univ. Press, Oxford, 1984).

[2]T. Udagawa and T. Tamura, Phys. Rev. C **29**, 1922 (1984).

[3]B. T. Kim, T. Udagawa, and T. Tamura, in *Proceedings of the International Conference on Fusion Reactions below the Coulomb Barrier, MIT, Cambridge, MA, 1984*, edited by S. Steadman (Springer, Berlin, 1984), p. 142; T. Tamura, T. Udagawa, and B. T. Kim, J. Phys. Soc. Jpn. **54**, Suppl. II, 40 (1985).

[4]T. Udagawa, B. T. Kim, and T. Tamura, Phys. Rev. C **32**, 124 (1985).

[5]See, for instance, a recent review article by J. R. Birkelund and J. R. Huizenga, Annu. Rev. Nucl. Part. Sci. **33**, 265 (1983).

[6]R. Vandenbosch *et al.*, Phys. Rev. C **28**, 1161 (1983).

[7]B. Haas *et al.*, Phys. Rev. Lett. **51**, 398 (1985).

[8]T. Tamura, Rev. Mod. Phys. **37**, 679 (1965).

[9]R. G. Stockstad and E. E. Gross, Phys. Rev. C **23**, 281 (1981).

[10]D. G. Sarantites *et al.*, Phys. Rev. C **14**, 2138 (1976), and references cited therein.